

Discerning and selectively manipulating laser-trapped atoms using non-paraxial light

R. Mitsch, C. Sayrin, B. Albrecht, P. Schneeweiss, and A. Rauschenbeutel*

*Vienna Center for Quantum Science and Technology,
Atominstitut, TU Wien, Stadionallee 2, 1020 Vienna, Austria*

(Dated: March 21, 2014)

We demonstrate that the non-paraxial character of a strongly confined light field can be used to spectrally discern and selectively manipulate two initially equivalent atomic ensembles of the same species. The technique is implemented with two symmetric linear arrays of cesium atoms, trapped on opposite sides of an optical nanofiber and separated by less than a micron. The nanofiber provides an evanescent field interface between the atoms and the guided light, where the latter exhibits a strongly position-dependent polarization. In the case of resonant interaction, this allows us to optically pump the ensembles into two distinct Zeeman states. In the case of dispersive interaction, the strong gradient of the light-induced fictitious magnetic field permits us to selectively address the ensembles with microwave radiation, thereby preparing them in distinct hyperfine states. This results in a composite fiber-coupled atomic medium with high potential for nonlinear optics at ultra-low light levels.

PACS numbers: 42.50.Ct, 37.10.Gh, 37.10.Jk, 42.25.Ja

Over the past decades, experimentalists have gained full control over the internal and external quantum degrees of freedom of individual quantum systems like single trapped ions [1] or atoms [2]. Coupling these quantum emitters to a single mode light field then allows one to, e.g., manipulate light at the quantum level [3], interconnect distant quantum systems [4], and prepare entangled states of light and matter [5, 6]. Extending these techniques to ensembles of atoms or ions gave rise to a wealth of interesting phenomena and applications, in particular in the context of efficient light-matter coupling [7] and the storage and retrieval of quantum states of light [8–10]. Discerning and selectively manipulating sub-classes of these ensembles with the same degree of control as achieved in the single particle case opens the route towards many protocols. For example, the interaction of light with an atomic medium consisting of two different classes of atoms allows one to tailor the dispersive and absorptive properties of the medium independently [11] and holds great promise for the realization of ultra-strong optical non-linearities down to the single photon level [12].

Nanofiber-based optical dipole traps, in which ensembles of a few thousand neutral atoms are trapped in the evanescent field surrounding a sub-wavelength-diameter silica fiber, have proven to provide an efficient interface between the nanofiber-guided light and the laser-cooled atoms [13, 14]. High optical depths of a few percent per atom have been demonstrated and nanofiber-trapped atoms have been coherently manipulated with coherence times in the millisecond range [15]. In conjunction with the waveguide geometry which provides a strong lateral confinement of the guided fields over the entire atomic sample, this system is thus ideally suited for the realization of linear and non-linear quantum optics schemes.

In this letter, we demonstrate that the non-paraxial character of the nanofiber-guided light can be used to spectrally discern and selectively manipulate two atomic

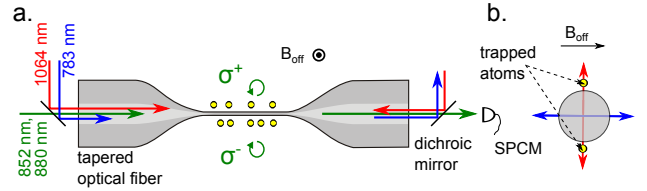


FIG. 1. **a.** Sketch of the experimental set-up including the tapered optical fiber, the laser fields, and the single-photon counting module (SPCM). The mostly circular polarization of the manipulation light fields (green line) at the position of the atoms (yellow dots) is indicated by the curved arrows and lies in the plane of the figure, denoted by \mathcal{P} . **b.** Cross-sectional view of the nanofiber displaying the orientation of the linear polarizations of the blue- and red-detuned trapping fields, the atoms, and the magnetic offset field.

ensembles that are simultaneously coupled to the fundamental nanofiber-guided mode. We first show that the two ensembles can be optically pumped to different ground states using only one laser field. We then demonstrate that by using light-induced fictitious magnetic fields [16] the ground state energy levels of the atoms can be shifted differently for the two ensembles, thereby enabling their independent coherent manipulation [17, 18]. The situation realized here is unique in the sense that the two atomic ensembles are initially perfectly equivalent in terms of their coupling to the nanofiber mode. Yet, this single field mode still can discern the ensembles without applying any external gradient fields thanks to its intrinsic polarization gradients.

The experimental setup is depicted in Fig. 1. Cesium atoms are trapped in the evanescent field surrounding an optical nanofiber (nominal radius $a = 250$ nm), realized as the waist of a tapered optical fiber (TOF). A blue-detuned running wave with a free-space wavelength of 783 nm and a power of 8.5 mW and a red-detuned

standing wave at 1064 nm wavelength with 0.77 mW per beam are sent through the TOF and create the trapping potential. Two diametric arrays of individual trapping sites are created 230 nm above the nanofiber surface [13]. The radial, azimuthal, and axial trap frequencies are 120, 87, 186 kHz, respectively. Each trapping site contains at most one atom, and the average filling factor is $\lesssim 0.5$ [19]. These two individual one-dimensional arrays, separated by $\lesssim 1 \mu\text{m}$, are a fraction of a millimeter long and correspond to two a priori equivalent atomic ensembles.

Any light field propagating in the optical nanofiber couples simultaneously to the two atomic ensembles. For all optical wavelengths involved in this experiment, the nanofiber only guides the fundamental HE_{11} mode [20]. Linearly polarized light that is coupled into this mode exhibits a significant non-zero longitudinal component of its electric field. The latter is $\pi/2$ -phase shifted with respect to the transverse components and its modulus and sign depend on the azimuthal position around the nanofiber [21]. The ellipticity vector $\epsilon = i(\mathcal{E} \times \mathcal{E}^*)/|\mathcal{E}|^2$, where \mathcal{E} is the positive-frequency envelope of the electric field, is thus position-dependent. In particular, $|\epsilon|$ is maximal along the direction of the transverse polarization of the light field and, for a wavelength of $\lambda = 852 \text{ nm}$ and at a distance of 230 nm from the nanofiber surface, reaches about 0.92. Moreover, ϵ has opposite signs on opposite sides of the fiber [22]. Hence, if the transverse polarization of the nanofiber-guided light lies in the plane \mathcal{P} containing the trapped atoms (see Fig. 1.a), \mathcal{E} is almost fully σ^+ polarized on one side of the nanofiber while it is almost fully σ^- polarized on the other side. Here, the quantization axis has been taken perpendicular to \mathcal{P} .

We demonstrate that this polarization pattern can be used to optically pump the trapped atoms in one of the two arrays into the outermost Zeeman sub-state $|F = 4, m_F = +4\rangle$ while the other array is pumped to $|F = 4, m_F = -4\rangle$. Once the atoms are loaded into the nanofiber-trap, they are in a mixture of m_F -states of the $F = 4$ hyperfine manifold [13]. We then apply a magnetic offset field \mathbf{B}_{off} of 28 G perpendicular to \mathcal{P} and send a manipulation light pulse through the TOF. The light pulse is resonant with the AC-Stark shifted $F = 4 \rightarrow F' = 5$ transition of the Cs D2 line ($\lambda = 852 \text{ nm}$) and its transverse polarization lies in \mathcal{P} . The frequency of the manipulation light is scanned over 135 MHz in 1 ms to address all m_F -states. The transmission spectrum of a subsequent probe pulse is recorded within 5 ms by a single-photon counting module and plotted as red dots in Fig. 2.b. The power of the manipulation and probe laser fields is 4 pW. Two resonances are clearly observed as two dips in the transmission spectrum. We fit the data with a generalized Beer-Lambert law [13] that takes into account two atomic transitions with a common linewidth Γ (solid lines in Fig. 2.b), and we find a very good agreement for the detunings $\Delta_{\text{probe}}^{(+)} = 39.82(8) \text{ MHz}$

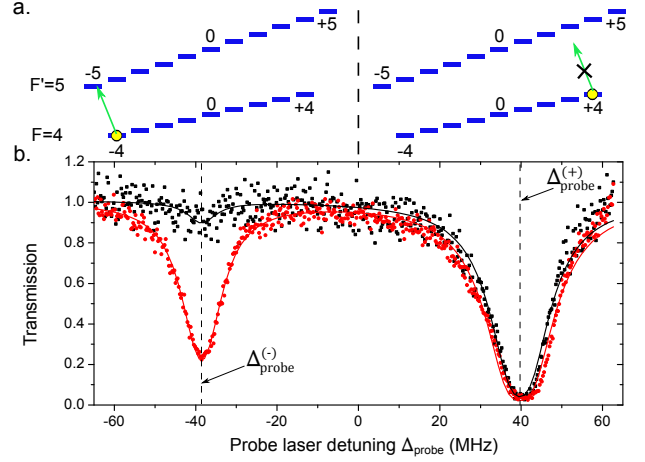


FIG. 2. **a.** Schematic of the energy levels of the trapped atoms. The yellow dots indicate the ideal population distribution of the two optically pumped atomic ensembles. The arrows indicate the transition driven by the push-out laser field which is resonant for the atoms on only one side of the fiber. **b.** Transmission spectrum of the probe light field recorded for $B_{\text{off}} = 28 \text{ G}$. The frequency is given relative to the measured resonance for $B_{\text{off}} = 0 \text{ G}$. The two absorption dips at $\Delta_{\text{probe}}^{(\pm)}$ stem from the two atomic arrays. The black (red) dots are recorded after (without) applying the push-out laser. The solid lines are fits to the data (see text).

and $\Delta_{\text{probe}}^{(-)} = -38.55(7) \text{ MHz}$ and for $\Gamma = 8.3(2) \text{ MHz}$. The fitted linewidth is slightly larger than the 5.2 MHz natural linewidth because of inhomogeneous light shifts induced by the trapping lasers. The frequency difference $\Delta_{\text{probe}}^{(+)} - \Delta_{\text{probe}}^{(-)} = 78.4(1) \text{ MHz}$ is in perfect agreement with the splitting between the outermost σ^+ and σ^- $F = 4 \rightarrow F' = 5$ transitions of 78.4 MHz for $B_{\text{off}} = 28 \text{ G}$ [23]. This confirms that, upon interaction with the manipulation field, the atoms in the two arrays are optically pumped towards the $|F = 4, m_F = +4\rangle$ and $|F = 4, m_F = -4\rangle$ states, respectively.

The demonstrated side-dependent optical pumping allows us to selectively address and, e.g., expel the atoms on only one side of the nanofiber from the trap. For this purpose, all atoms are exposed for 5 ms to a σ^- -polarized push-out laser beam [24] that is resonant with the AC-Stark shifted $|F = 4, m_F = -4\rangle \rightarrow |F' = 5, m_F = -5\rangle$ transition (Fig. 2.a) and that propagates along \mathbf{B}_{off} . The probe transmission spectrum is then measured as before, after an additional 1 ms-long optical pumping sequence, see black line in Fig. 2.b. While the dip at $\Delta_{\text{probe}}^{(+)}$ has not been significantly affected by the push-out laser, the dip at $\Delta_{\text{probe}}^{(-)}$ is now barely visible: Atoms are expelled from the trap on one side and remain trapped on the other side of the nanofiber. This technique is particularly useful if one wants to couple trapped atoms to other quantum devices, such as SQUIDs [25] or photonic structures: Knowing on which side of the fiber the atoms

are prepared gives one full control over their position [26] with respect to the device.

We now show that it is possible to discern and to individually manipulate the ensembles even when prepared in the same Zeeman substate. This would allow one, for example, to work with both ensembles in the least magnetic field-sensitive $|F, m_F = 0\rangle$ states in order to reach long coherence times [15]. For this purpose, we make the transition frequencies between the hyperfine ground states for the two atomic arrays different. This is achieved using the m_F -state-dependent AC Stark shift induced by a far-detuned nanofiber-guided field: The AC Stark shift of the alkali atom ground states can be decomposed into an m_F -state-independent scalar and an m_F -state-dependent vector part [27]. The latter can be expressed as the effect of a fictitious magnetic field [16]

$$\mathbf{B}_{\text{fict}} = \beta^{(v)} i \boldsymbol{\mathcal{E}} \times \boldsymbol{\mathcal{E}}^* = \beta^{(v)} |\boldsymbol{\mathcal{E}}|^2 \boldsymbol{\epsilon}, \quad (1)$$

where $\beta^{(v)}$ is proportional to the vector polarizability of the Cs ground state [27]. Like for the ellipticity vector, $|\mathbf{B}_{\text{fict}}|$ is maximal along the direction of transverse polarization and \mathbf{B}_{fict} has opposite signs on opposite sides of the fiber [21]. Thus, in the presence of an additional detuned nanofiber-guided light field, the two atomic arrays are subjected to opposite fictitious magnetic fields which are maximized if the polarization of this light field lies in \mathcal{P} (see Fig. 3.a). The linear Zeeman effect then leads to the desired lift of degeneracy between the two nanofiber sides for first order magnetic field sensitive transitions. In the case of transitions that only exhibit a quadratic Zeeman shift, like the $|F = 3, m_F = 0\rangle \rightarrow |F = 4, m_F = 0\rangle$ hyperfine clock transition, a non-zero external offset field \mathbf{B}_{off} must be applied in order to make the modulus of the total magnetic field side-dependent and thus to lift the degeneracy. In Fig. 3.b, we depict this situation for $\mathbf{B}_{\text{off}} \perp \mathcal{P}$ and $B_{\text{off}} > B_{\text{fict}}$. At the positions of the two atomic arrays, we then have $|\mathbf{B}_{\text{off}} + \mathbf{B}_{\text{fict}}| = B_{\text{off}} \pm B_{\text{fict}}$.

While the light-induced fictitious magnetic field can be used to make the transition frequencies side-dependent, one has to avoid a significant distortion of the trapping potential by an unwanted scalar shift that is induced by the same laser: The strong radial intensity gradient of the nanofiber-guided fields [28] results in a corresponding gradient of this scalar shift that leads to additional dipole forces. It is, however, possible to circumvent this problem by a proper choice of the wavelength of the laser that induces \mathbf{B}_{fict} . First, we can operate the laser at a tune-out wavelength [29], for which the scalar shift of the ground states vanishes. And second, \mathbf{B}_{fict} can be induced by one of the trapping lasers. In the trapping configuration of Fig. 1, the fictitious magnetic fields induced by the red and blue trapping fields vanish at the position of the trapping minima. However, a slight modification of the imbalance between the two counter-propagating red fields or a tilt of the blue polarization by a small angle from its initial position results in $B_{\text{fict}} \neq 0$ because the

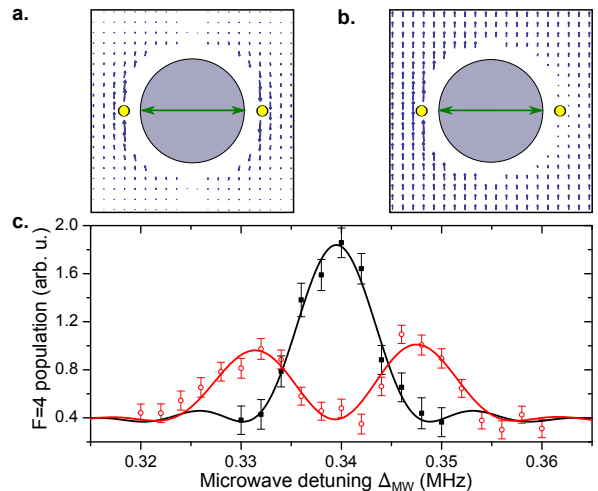


FIG. 3. **a.**, **b.** Cross-sectional view of the nanofiber indicating the position of the atoms (yellow dots) and the magnetic field $\mathbf{B}_{\text{off}} + \mathbf{B}_{\text{fict}}$ (blue arrows), where \mathbf{B}_{fict} is the fictitious magnetic field induced by a detuned quasi-linearly polarized light field (green double arrow): **a.** $B_{\text{off}} = 0$, **b.** $B_{\text{off}} > B_{\text{fict}}$. **c.** Population of the $F = 4$ manifold after a 103 μs -long MW pulse that transfers atoms which are initially in $|F = 3, m_F = 0\rangle$ to $|F = 4, m_F = 0\rangle$, as a function of the frequency of the MW source ($B_{\text{off}} = 28 \text{ G}$). The frequency is given relative to the zero-field clock transition frequency in free space. The black squares (red circles) have been obtained without (with) sending the tune-out laser through the nanofiber. The solid lines are fits using a Fourier-limited line shape.

polarization at the position of the atoms becomes elliptical [21]. At the same time, this does not significantly modify the scalar shift and thus leaves the trapping potential essentially unchanged.

We first characterize the effect of a nanofiber-guided manipulation light field at the Cs tune-out wavelength of 880.2524 nm on the clock transition of the two atomic arrays. We use a tunable microwave (MW) source at 9.2 GHz that drives transitions between the hyperfine ground states. The black squares in Fig. 3.c show the measured MW spectrum in the presence of a magnetic offset field $B_{\text{off}} = 28 \text{ G}$ without applying the manipulation light field. For this measurement, the atoms are first prepared in the $F = 3$ manifold. A 103- μs long MW π -pulse is then applied and transfers the atoms that are initially in $|F = 3, m_F = 0\rangle$ to the $|F = 4, m_F = 0\rangle$ state. Finally, the population of the $F = 4$ manifold is measured as in [15] and plotted as a function of the MW detuning Δ_{MW} . A single Fourier limited peak is observed, see black line: in this configuration, the two atomic ensembles are equivalent and contribute equally to the measured spectrum.

The red circles in Fig. 3.c show the MW spectrum under the same conditions when applying the manipulation light field with a power of 100 μW . A clear splitting of the resonance of 16.6(6) kHz is observed which we identify as

the difference of the quadratic Zeeman shifts of the two atomic ensembles. Here, we enhanced the splitting by working with $B_{\text{off}} \gg B_{\text{fict}}$. In this regime, the frequency shifts of the clock transition are approximately given by $\alpha_0 (B_{\text{off}}^2 \pm 2B_{\text{off}} \cdot B_{\text{fict}})$, where $\alpha_0 = 0.427 \text{ kHz/G}^2$ [23], so that the splitting becomes linear in B_{fict} and is proportional to B_{off} . Moreover, this implies that the two transition frequencies should split symmetrically with respect to the case without manipulation light field. This is in agreement with our experimental observations, see Fig. 3.c. From the measured splitting in conjunction with the strength of the offset field, we find $B_{\text{fict}} = 0.35 \text{ G}$ at the position of the atoms. Taking into account the distance of about $1 \mu\text{m}$ between the atomic arrays, this corresponds to a gradient of B_{fict} of 70 T/m , one order of magnitude larger than what was previously achieved with light induced fictitious magnetic fields [17].

The above technique has the advantage that the splitting of the transition frequencies of the two atomic ensembles can be varied as fast as one can modulate the optical power of the manipulation light field. However, we experimentally observed that large splittings come at the expense of a broadening of the hyperfine transition. We attribute this fact to the strong gradient of B_{fict} (see Fig. 3.a) which leads to position-dependent level-shifts and thus to a distortion of the trap. In particular, calculations show that the radial position of the trapping minima of the two hyperfine states are displaced in opposite directions. As a consequence, for $m_F = \pm 3$ states, whose coherence times are an order of magnitude smaller than those of the $m_F = 0$ states in our experiment, the MW spectrum is significantly altered when inducing frequency splittings that are large enough to be resolved.

We now characterize the scheme that relies on tilting the transverse polarization of the blue trapping field by a small angle φ_B for introducing the fictitious magnetic field at the position of the atoms. We analyze the first-order magnetic-field sensitive $|F=3, m_F=-3\rangle \rightarrow |F=4, m_F=-3\rangle$ transition for three different values of φ_B . To this end, we combine the two experimental techniques that were used to obtain the results shown in Figs. 2 and 3: Following a $40\text{-}\mu\text{s}$ long MW π -pulse with $B_{\text{off}} = 3 \text{ G}$, we increase the offset field to 28 G and perform a 1-ms long optical pumping sequence. We then record the probe laser transmission in dependence of the MW detuning, Δ_{MW} , and the probe laser detuning, Δ_{probe} . The resulting spectra are displayed as density plots in Fig. 4.a–c. For each tilt angle, we observe two transmission minima at two different probe laser detunings which correspond, as in Fig. 2, to the two atomic ensembles on the two sides of the nanofiber. For $\varphi_B = 0$, the transmission minima occur for the same MW detuning. For $\varphi_B = 5^\circ$, however, the two minima appear at different values of Δ_{MW} , corresponding to a splitting of $31.1(8) \text{ kHz}$. This splitting further increases to $60.7(9) \text{ kHz}$ for $\varphi_B = 8^\circ$. This is almost four

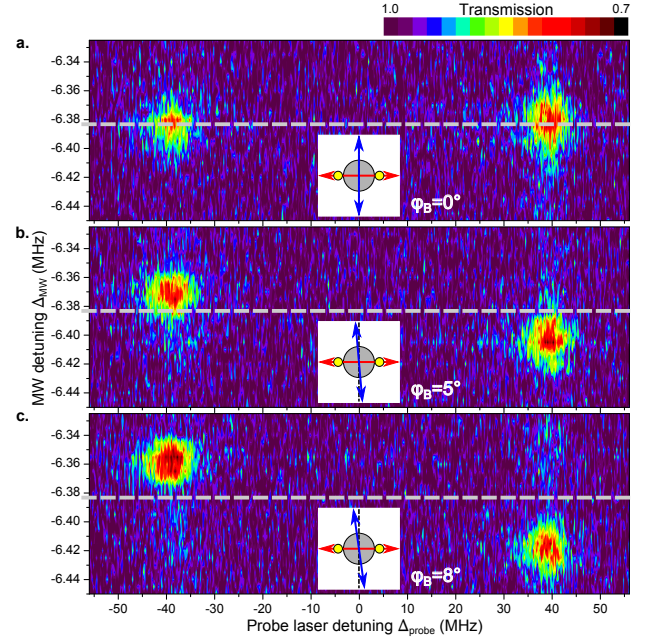


FIG. 4. Probe laser transmission in dependence of the MW detuning, Δ_{MW} , and the probe laser detuning, Δ_{probe} , for different values of the tilt angle, φ_B , of the blue detuned trapping light field: **a.** $\varphi_B = 0^\circ$, **b.** $\varphi_B = 5^\circ$, **c.** $\varphi_B = 8^\circ$. The dashed line indicates the resonant MW detuning when $\varphi_B = 0^\circ$.

times larger than what was achieved with the manipulation light field at the tune-out wavelength. In particular, even with the first-order magnetic field sensitive transition used here, this allowed us to clearly spectrally discern the two atomic ensembles, see Fig. 4.c.

In summary, we showed that the strongly non-paraxial character of nanofiber-guided light can be used to discern and to selectively manipulate two individual nanofiber-trapped atomic ensembles. Taking advantage of the strong polarization gradients of the fundamental nanofiber mode, side-dependent optical pumping was realized and allowed us to prepare the two ensembles in different Zeeman sub-states. Moreover, the associated light-induced fictitious magnetic fields were utilized to lift the degeneracy of the Zeeman sub-states for the two atomic ensembles by a few 10 kHz . This made it possible to selectively address the two ensembles with MW radiation and to independently prepare them in different hyperfine states. The presented techniques allow us to realize a composite atomic medium as considered in [12], where the propagation of two light fields under the condition of electromagnetically induced transparency would enable a non-linear interaction between single fiber-guided photons. Finally, given that our method exploits the intriguing properties of non-paraxial light fields, it can be extended to many other quantum optical systems that operate in the non-paraxial regime, like atoms coupled to plasmonic structures [30], to nanophotonic devices [31, 32], or to optical microtraps [33, 34].

We acknowledge financial support by the Austrian Science Fund (FWF, SFB NextLite project No. F 4908-N23 and DK CoQuS project No. W 1210-N16). C.S. acknowledges support by the European Commission (Marie Curie IEF Grant 328545). R. M. and C. S. contributed equally to this work.

* Arno.Rauschenbeutel@ati.ac.at

- [1] D. J. Wineland, Rev. Mod. Phys. **85**, 1103 (2013).
- [2] D. Meschede and A. Rauschenbeutel, Advances in Atomic, Molecular, and Optical Physics **53**, 75 (2006).
- [3] S. Haroche, Rev. Mod. Phys. **85**, 1083 (2013).
- [4] S. Ritter, C. Nölleke, C. Hahn, A. Reiserer, A. Neuzner, M. Uphoff, M. Mücke, E. Figueroa, J. Bochmann, and G. Rempe, Nature **484**, 195 (2012).
- [5] B. B. Blinov, D. L. Moehring, L.-M. Duan, and C. Monroe, Nature **428**, 153 (2004).
- [6] J. Volz, M. Weber, D. Schlenk, W. Rosenfeld, J. Vrana, K. Saucke, C. Kurtsiefer, and H. Weinfurter, Phys. Rev. Lett. **96**, 030404 (2006).
- [7] K. Hammerer, A. S. Sørensen, and E. S. Polzik, Rev. Mod. Phys. **82**, 1041 (2010).
- [8] K. S. Choi, H. Deng, J. Laurat, and H. J. Kimble, Nature **452**, 67 (2008).
- [9] A. I. Lvovsky, B. C. Sanders, and W. Tittel, Nat. Phot. **3**, 706 (2009).
- [10] K. Jensen, W. Wasilewski, H. Krauter, T. Fernholz, B. M. Nielsen, M. Owari, M. B. Plenio, A. Serafini, M. M. Wolf, and E. S. Polzik, Nat. Phys. **7**, 13 (2011).
- [11] N. A. Proite, B. E. Unks, J. T. Green, and D. D. Yavuz, Phys. Rev. Lett. **101**, 147401 (2008).
- [12] M. D. Lukin and A. Imamoglu, Phys. Rev. Lett. **84**, 1419 (2000).
- [13] E. Vetsch, D. Reitz, G. Sagué, R. Schmidt, S. T. Dawkins, and A. Rauschenbeutel, Phys. Rev. Lett. **104**, 203603 (2010).
- [14] A. Goban, K. S. Choi, D. J. Alton, D. Ding, C. Lacroûte, M. Pototschnig, T. Thiele, N. P. Stern, and H. J. Kimble, Phys. Rev. Lett. **109**, 033603 (2012).
- [15] D. Reitz, C. Sayrin, R. Mitsch, P. Schneeweiss, and A. Rauschenbeutel, Phys. Rev. Lett. **110**, 243603 (2013).
- [16] C. Cohen-Tannoudji and J. Dupont-Roc, Phys. Rev. A **5**, 968 (1972).
- [17] N. Lundblad, J. M. Obrecht, I. B. Spielman, and J. V. Porto, Nat. Phys. **5**, 575 (2009).
- [18] C. Weitenberg, M. Endres, J. F. Sherson, M. Cheneau, P. Schauß, T. Fukuhara, I. Bloch, and S. Kuhr, Nature **471**, 319 (2011).
- [19] E. Vetsch, S. Dawkins, R. Mitsch, D. Reitz, P. Schneeweiss, and A. Rauschenbeutel, IEEE J. Sel. Top. Quant. Electron. **18**, 1763 (2012).
- [20] A. W. Snyder and J. D. Love, *Optical Waveguide Theory* (Chapman and Hall, New York, 1983).
- [21] Fam Le Kien, P. Schneeweiss, and A. Rauschenbeutel, Phys. Rev. A **88**, 033840 (2013).
- [22] D. Reitz, C. Sayrin, B. Albrecht, I. Mazets, R. Mitsch, P. Schneeweiss, and A. Rauschenbeutel, ArXiv e-prints (2014), arXiv:1402.3265 [physics.atom-ph].
- [23] D. Steck, *Cesium D Line Data* (available online at <http://steck.us/alkalidata>, 2010).
- [24] S. Kuhr, W. Alt, D. Schrader, I. Dotsenko, Y. Miroshnychenko, A. Rauschenbeutel, and D. Meschede, Phys. Rev. A **72**, 023406 (2005).
- [25] M. Hafezi, Z. Kim, S. L. Rolston, L. A. Orozco, B. L. Lev, and J. M. Taylor, Phys. Rev. A **85**, 020302 (2012).
- [26] P. Schneeweiss, S. T. Dawkins, R. Mitsch, D. Reitz, E. Vetsch, and A. Rauschenbeutel, Applied Physics B **110**, 279 (2013).
- [27] Fam Le Kien, P. Schneeweiss, and A. Rauschenbeutel, The European Physical Journal D **67**, 1 (2013).
- [28] Fam Le Kien, J. Liang, K. Hakuta, and V. Balykin, Optics Communications **242**, 445 (2004).
- [29] B. Arora, M. S. Safronova, and C. W. Clark, Phys. Rev. A **84**, 043401 (2011).
- [30] C. Stehle, H. Bender, C. Zimmermann, D. Kern, M. Fleischer, and S. Slama, Nat. Phot. **5**, 494 (2011).
- [31] J. D. Thompson, T. G. Tiecke, N. P. de Leon, J. Feist, A. V. Akimov, M. Gullans, A. S. Zibrov, V. Vuletic, and M. D. Lukin, Science **340**, 1202 (2013).
- [32] A. Goban, C.-L. Hung, S.-P. Yu, J. D. Hood, J. A. Muniz, J. H. Lee, M. J. Martin, A. C. McClung, K. S. Choi, D. E. Chang, O. Painter, and H. J. Kimble, ArXiv e-prints (2013), arXiv:1312.3446 [physics.optics].
- [33] A. M. Kaufman, B. J. Lester, and C. A. Regal, Phys. Rev. X **2**, 041014 (2012).
- [34] J. D. Thompson, T. G. Tiecke, A. S. Zibrov, V. Vuletic, and M. D. Lukin, Phys. Rev. Lett. **110**, 133001 (2013).